crystals

MDPI

Article

Structure of a Novel Spinel $Li_{0.5}Zn_{5/3}Sb_{2.5/3}O_4$ by Neutron and Synchrotron Diffraction Analysis

José Alfredo Marín-Romero [1,*], Luis Edmundo Fuentes-Cobas [2], Juan Rodríguez-Carvajal [3], Carolina Tabasco-Novelo [1] and Patricia Quintana [1]

1 Department of Applied Physics, CINVESTAV IPN Unidad-Mérida, Mérida 97310, Mexico; carolina.tabasco@cinvestav.mx (C.T.-N.); pquint@cinvestav.mx (P.Q.)
2 Advanced Materials Research Center, Chihuahua 31000, Mexico; luis.fuentes@cimav.edu.mx
3 Institut Laue Langevin, CS 20156, 38042 Grenoble, Cedex 9, France; rodriguez-carvajal@ill.fr
* Correspondence: jose.marin@cinvestav.mx; Tel.: +52(999)-942-9442

Academic Editor: William Clegg
Received: 27 July 2017; Accepted: 12 September 2017; Published: 15 September 2017

Abstract: $Zn_{7/3}Sb_{2/3}O_4$ is a secondary phase in ZnO-based varistors. Acceptor impurities, such as Li^+, increase the resistivity. This effect is produced by a modification of the grain boundary barriers. The role of the cationic distribution in the mentioned events is worth clarifying. The $Li_{0.5}Zn_{5/3}Sb_{2.5/3}O_4$ room-temperature structure was determined by means of a neutron diffraction and synchrotron X-ray diffraction investigation. The title compound was prepared by conventional ceramic process. The elemental composition of the investigated sample was verified by means of electron microscopy—energy dispersive X-ray spectroscopy and X-ray photoelectron spectroscopy. The neutron experiment was performed at the high-intensity neutron diffractometer with position-sensitive detector at the D1B beamline of the Laue-Langevin Institute, Grenoble. The high resolution synchrotron measurement was carried out at MCX beamline of Elettra Sincrotrone Trieste. Rietveld analysis was performed with the FullProf program. $Li_{0.5}Zn_{5/3}Sb_{2.5/3}O_4$ belongs to the spinel family, space group $Fd\overline{3}m$ (227). The measured lattice parameter is a = 8.5567(1) Å. The Li^{+1} and Zn^{+2} ions are randomly distributed among the tetrahedral and octahedral sites as opposed to Sb^{+5} ions which have preference for octahedral sites. Fractional coordinate of oxygen, u = 0.2596(1), indicates a slight deformation of the tetrahedral and octahedral sites. The data given in this paper provide structural support for further studies on measurements and microscopic explanations of the interesting properties of this family of compounds.

Keywords: spinel; varistors; $Zn_7Sb_2O_{12}$; Rietveld analysis; neutron diffraction; synchrotron radiation

1. Introduction

Spinels motivate continuous scientific interest due to their physicochemical properties and their application in a wide spectrum of fields. They are used in catalysis, power management, telecommunications, medicine, and physical-chemical sensing, among other disciplines [1–6].

An important current field of spinel application is as a component of multiphase systems, such as ZnO ceramic varistors, to which small amounts of (Bi, Sb, Co, Mn, Cr, Al, Ni) oxides are added to improve their electrical characteristics. Particularly zinc antimony spinel, $Zn_{7/3}Sb_{2/3}O_4$, is a well-known secondary phase in ZnO-based varistor ceramics. It has been reported to inhibit ZnO grain growth and to diminish the sintering temperature, therefore attaining better stability at higher voltages. The mentioned effect is due to segregation effects at grain boundaries, leading to the formation of separate spinel grains. The electrical properties of Zn-based spinels are sensitive to variations in the crystallographic structure [7–9].

Undoped $Zn_{7/3}Sb_{2/3}O_4$ has two polymorphic phases. According to Harrington [10], the transition from the low-temperature β-polymorph to the high-temperature α-polymorph occurs at 1225 °C. The α-phase is cubic inverse spinel [11–13]. Its configuration shows 8 tetrahedral positions occupied by Zn and 16 octahedral sites randomly occupied by Sb and Zn. The occupancy ratio of Sb and Zn at the octahedral positions is 1:2 [14]. The geometry of the structural tetrahedra and octahedra vary weakly with changes in environmental and crystallization conditions [15]. The β-phase adopts a complex orthorhombic structure [10,16], possibly forming a superstructure [17].

It has been published that a small addition (ppm order) of monovalent cations—such as Li^+, Na^+, or K^+—to $Zn_{7/3}Sb_{2/3}O_4$ has an influence on the ZnO varistors' electric properties, presumably because it acts as a grain growth inhibitor, decreases the donor density, and thus increases the potential barrier. In addition, the small size effect facilitates the diffusion of lithium cations into the ZnO crystal lattice [18–20].

Studying the binary system $Zn_{7/3}Sb_{2/3}O_4$–$LiZnSbO_4$, we have found the formation of a solid solution $Li_xZn_{(7-4x)/3}Sb_{(2+x)/3}O_4$ ($0.3 < x < 0.6$). Therefore, the aim of the present study is to determine the crystal structure of characteristic compound $Li_{0.5}Zn_{1.67}Sb_{0.83}O_4$ ($x = 0.5$) with focus on the elucidation of the ionic distribution. The investigation was performed by means of neutron diffraction (ND) and synchrotron X-ray diffraction (SyXRD).

2. Experimental

Polycrystalline $Li_{0.5}Zn_{5/3}Sb_{2.5/3}O_4$ was prepared by solid-state reaction process. The purity of the compounds was as follows: (1) Li_2CO_3 (99.99% Sigma Aldrich, St. Louis, MO, USA) dehydrated at 600 °C, (2) ZnO (99.99% Sigma Aldrich) dehydrated at 200 °C, and (3) Sb_2O_5 (99.95% Sigma Aldrich). The compounds were ground in an agate mortar with acetone to favor a homogeneous mixture and then heated in Pt foil boats up to a temperature of 750 °C for six hours to achieve decarbonation of Li_2CO_3. The final heat treatment consisted of a five-cycle process, with 24 h per cycle, at rising temperatures from 800 °C to 1000 °C (ΔT = 50 °C per cycle), in normal oxidizing atmosphere. At the end of every heat treatment the sample was removed from the furnace and cooled in air, weighed, and reground prior each treatment. In order to confirm the formation of the desired phase, the obtained sample was characterized by means of conventional XRD.

To verify the elemental composition of the investigated sample, a scanning electron microscopy–energy dispersive X-ray spectroscopy (SEM-EDXS) observation was performed using a JEOL JSM-7600F (JEOL, Tokyo, Japan). X-ray photoelectron spectroscopy (XPS) was carried out in a Thermo Scientific K-alpha (Thermo Fisher Scientific, East Grinstead, England), in ultrahigh vacuum with a monochromatic Al Kα X-ray source with an energy of 1486.6 eV.

High resolution SyXRD experiment was carried out at MCX beamline of Elettra Sincrotrone Trieste (Trieste, Italy). Taking into consideration the output spectrum of the MCX beamline, the value E = 13.048 keV, leading to λ = 0.9500 Å was chosen. The experimental setup was calibrated by the measurement of a silicon standard. The sample was measured with reflection geometry on a flat sample-holder plate. The measured angular domain was $10° < 2\theta < 90°$, with a recording step of $\Delta(2\theta) = 0.005°$.

The ND experiment was carried out on the high-intensity D1B beamline of the Laue–Langevin Institute, Grenoble. The sample was measured inside of a vanadium tube with a position sensitive detector diffractometer, with 0.1° step in 2θ, in a range of $1° \leq 2\theta \leq 128°$, with λ = 1.28 Å.

The structural refinement of $Li_{1.5}Zn_5Sb_{2.5}O_{12}$ was carried out using FullProf program [21]. In a first stage of refinement, the scale factor, zero error, and background were adjusted. Next, lattice parameters, profile, and structural data were refined. Within the adopted structural model, the only atomic coordinates adjusted were the oxygen fractional coordinates. The Debye-Waller factors were treated as isotropic. Two restraints were considered. The first one is that the tetrahedral and octahedral spaces are fully occupied and the second one is that the antimony ions are located at the octahedral sites [22–25].

3. Results and Discussion

The $Li_{0.5}Zn_{5/3}Sb_{2.5/3}O_4$ compound shows spinel structure, as described in Figure 1. The space group is $Fd\overline{3}m$ (227) and the lattice parameter is a = 8.5567(1) Å. Crystal data and structure refinement details of the Rietveld refinements of ND and SyXRD were combined and summarized in Table 1. Figure 2 shows the Rietveld refinement of the ND study, in which the ionic distributions were adjusted. Figure 3 shows the SyXRD Rietveld refinement, focused on the lattice parameters determination.

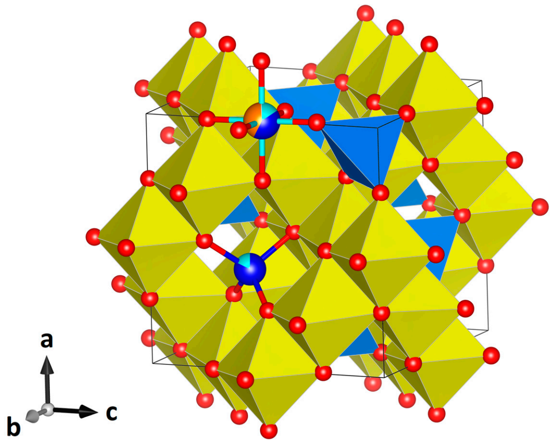

Figure 1. Spinel structure of $Li_{0.5}Zn_{1.67}Sb_{0.83}O_4$. The different colors in the spheres represent the degree of occupation of each element. O (red), Li (green), Zn (blue), and Sb (brown). The polyhedra are centered at the octahedral and tetrahedral sites.

Table 1. Crystallographic data and refinement of the compound $Li_{0.5}Zn_{5/3}Sb_{2.5/3}O_4$.

Crystal Data					
			Radiation		
Cubic, $Fd\overline{3}m$ (227)			Synchrotron X-rays, λ = 0.9500 Å		
			Constant wavelength Neutron, λ = 1.28 Å		
a = 8.5567(1) Å			Particle morphology: equiaxial powder		
V = 626.5078(2) $Å^3$			Color: White		
Z = 8					
Rietveld reliability factors					
ND Data			XRD Data		
R_p = 0.05			R_p = 0.06		
R_{wp} = 0.06			R_{wp} = 0.08		
R_{exp} = 0.05			R_{exp} = 0.05		
R_{Bragg} = 3.928			R_{Bragg} = 5.377		
χ^2 = 1.631			χ^2 = 4.0342		
1150 data points			9794 data points		
Excluded region(s): none			Excluded region(s): 1 (23° ≤ 2θ ≤ 24°)		
	x	y	z	U_{iso}	*Occupancy*
Zn1	0.12500	0.12500	0.12500	0.0107(10)	0.82(4)
Li1	0.12500	0.12500	0.12500	0.0107(10)	0.18(4)
Li2	0.50000	0.50000	0.50000	0.0121(6)	0.16(2)
Zn2	0.50000	0.50000	0.50000	0.0121(6)	0.42(2)
Sb1	0.50000	0.50000	0.50000	0.0121(6)	0.42(2)
O1	0.2596(1)	0.2596(1)	0.2596(1)	0.0131(3)	

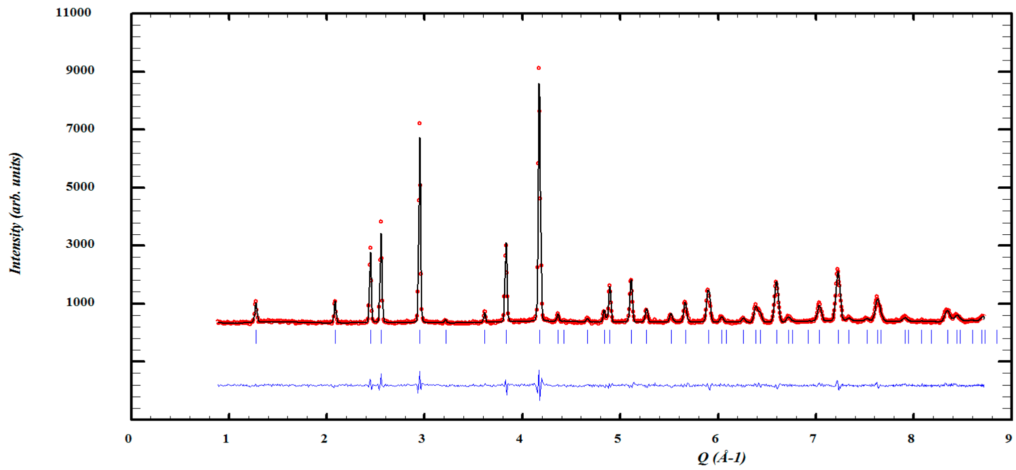

Figure 2. Observed and calculated ND diffraction patterns of $Li_{0.5}Zn_{1.67}Sb_{0.83}O_4$. Measurement statistics, background level, Q interval, and refinement reliability factors are in the usual range.

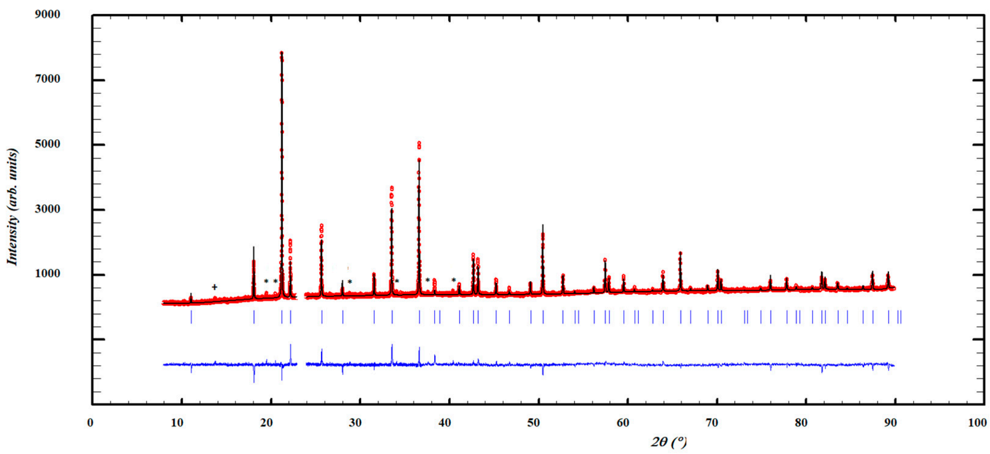

Figure 3. Observed and calculated SyXRD diffraction patterns of $Li_{0.5}Zn_{1.67}Sb_{0.83}O_4$. The diagram shows traces (~1%) of Li_8PtO_6 (+) and ZnO (*). The small interval around $2\theta \approx 24°$ was not taken into consideration. It showed a strong peak from the sample holder.

The material SEM observation is shown in Figure 4a,b. Observed particles show regular morphologies, with smooth surfaces and defined edges; the particle sizes are around 200 nm. Figure 4c shows the elemental analysis by EDXS of a representative area; the atomic percentage ratio for Zn:Sb is 2:1, in agreement with the given significant figures in the $Li_{0.5}Zn_{1.67}Sb_{0.83}O_4$ formula. The assumption of total occupation for the tetrahedral and octahedral sites is consistent with the compound electrical neutrality and the obtained refinement reliability coefficients. Further, the cation Sb^{5+} has the electronic configuration as $t_{2g}^6\ e_g^2$, which leads to octahedral occupancy.

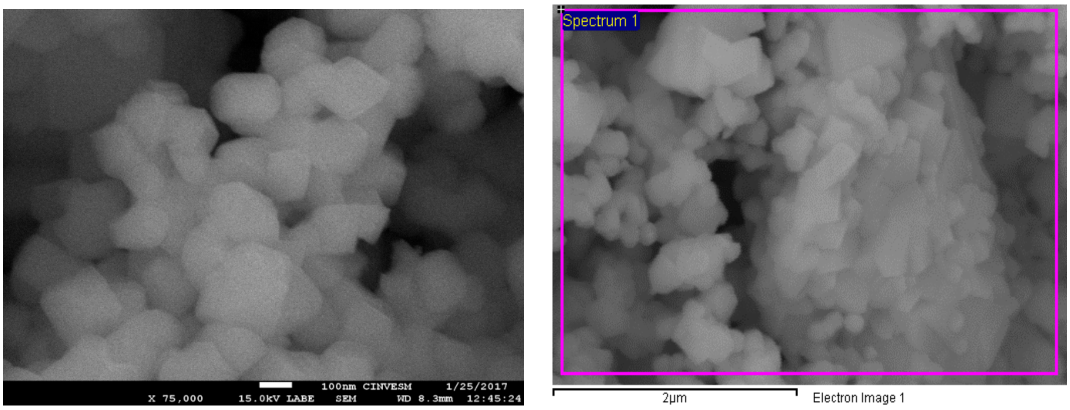

(**a**) (**b**)

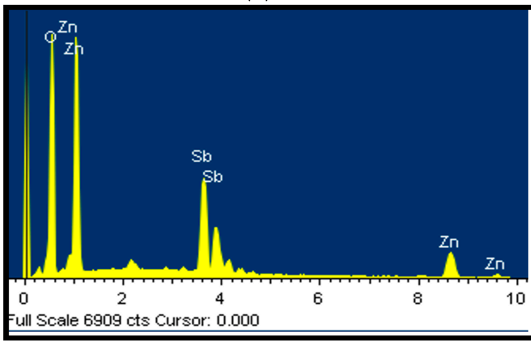

Element	Weight%	Atomic%
O K	26(1)	66(1)
Zn K	37.6(2)	22.6(6)
Sb L	36.4(7)	11.4(4)
Total	100.00	100.00

(**c**)

Figure 4. (**a**) SEM observation of particles morphology. (**b**) Representative area for The EDXS measurement. Approximate dimensions: 4 × 3 µm^2. (**c**) EDXS elemental analysis.

Further evidence of the composition of the sample was obtained from XPS analysis. The binding energies were corrected for specimen charging to the carbon C 1s position at 284.8 eV. C 1s line came from adventitious surface carbon. The XPS spectrum of $Li_{1.5}Zn_5Sb_{2.5}O_{12}$ powder (Figure 5a), confirms the presence of zinc, antimony, lithium, and oxygen. O 1s and Sb $3d_{5/2}$ peaks are overlapped. They have similar binding energies of 539.28 eV and 539.48 eV, respectively (Figure 5c). To circumvent the mentioned obstacle, the Sb concentration was determined via the Sb $3d_{3/2}$ peak (530.07 eV) [6,26,27]. The high-resolution spectra for Zn 2p, Sb $3d_{3/2}$, O 1s, and Li 1s are shown in Figure 5b–d. The atomic concentrations were calculated by means of Equation (1)

$$C_x = \frac{I_x/S_x}{\sum_i I_i/S_i} \quad (1)$$

C_x and I_x are, respectively, the atomic fraction and the peak area of element x and S_x is the relative sensitivity of the considered photoelectron peak [28]. The atomic percentage for each element was Li (7.3%), Zn (22.4%), Sb (12.7%), and O (57.6%) which are in a good agreement with the composition of $Li_{1.5}Zn_5Sb_{2.5}O_{12}$.

The lattice parameter of the investigated phase is larger than that of the spinel $Li_{0.64}Fe_{2.15}Ge_{0.21}O_4$ (a = 8.2903(3) Å) [29], similar to $Zn_2Co_5Sb_2O_{12}$ (a = 8.55917(9) Å) and smaller than the ones of spinel $Zn_7Sb_2O_{12}$ (a = 8.6047 Å) [16].

The site-occupation refinement indicates that Li^+ and Zn^{+2} are distributed on tetrahedral and octahedral sites. In the work of Harrington for $Zn_7Sb_2O_{12}$ doped with Cr and Ni, Zn^{+2} was located only in tetrahedral positions [6,12]. However, Ezhilvalavan & Kutty reported that Zn^{2+} ions are located in both octahedral and tetrahedral positions [30].

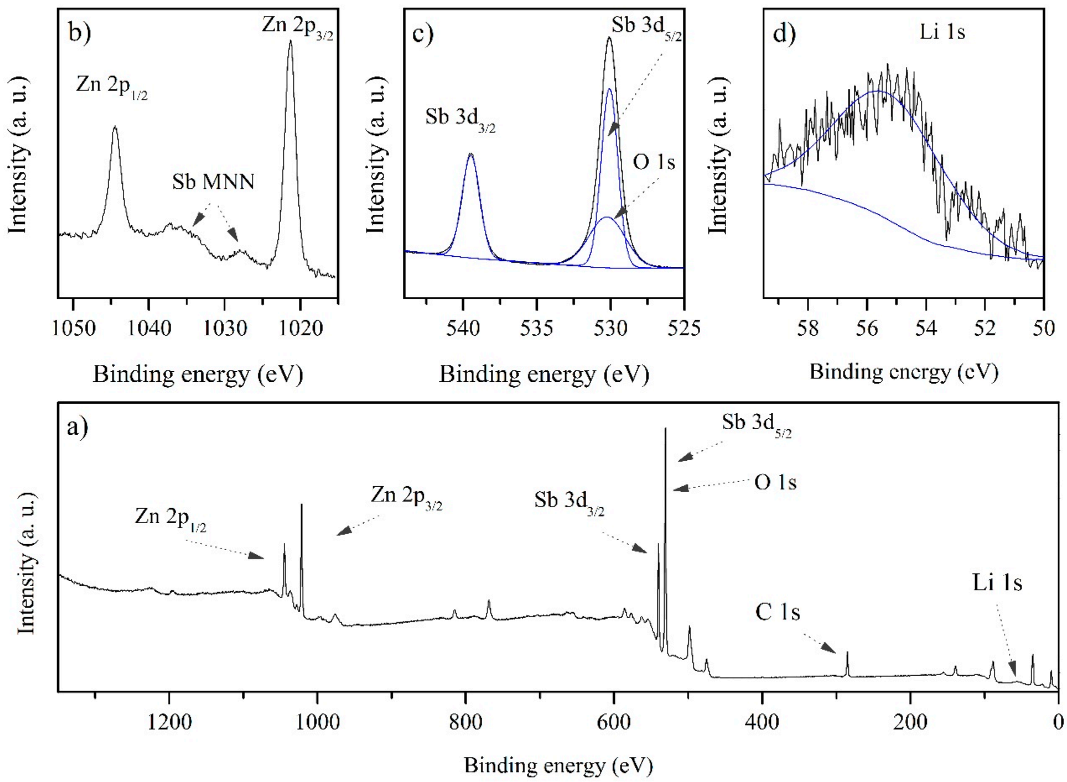

Figure 5. XPS spectrum for (**a**) $Li_{1.5}Zn_5Sb_{2.5}O_{12}$ and high-resolution spectra (**b**–**d**) for Zn, Sb, O, and Li, respectively.

The determined value of the oxygen fractional coordinate (u = 0.2596(1)) is slightly higher than the ideal spinel value. To explore the geometrical implications of this result, the cation–oxygen distances were calculated by means of the program Vesta [31] and by the equations of O'Niell and Talanov [1,32]. Our geometrical results are compared with those reported by other authors and with the ones calculated by mean of the Shannon radii, weighting with the occupation factors. The values obtained via Shannon radii were b_t(Shannon) = 1.998 Å and b_o(Shannon) = 2.088 Å. Our experimental bond length in the tetrahedral sites is b_t = 1.986(4) Å. This value is comparable with those of $Zn_2Co_5Sb_2O_{12}$ (b_t = 1.99807(2) Å) [16], $Zn_{7/3}Sb_{2/3}O_4$ (b_t = 2.015(8) Å) [10] and $Li_{0.64}Fe_{2.15}Ge_{0.21}O_4$ (b_t = 1.857(2) Å) [29]. In the octahedral sites, the bond length is b_o = 2.065(4) Å. Our value is slightly less than those corresponding to the aforementioned reports by Redhammer and Harrington (b_o = 2.0373(11)) Å [29]; b_o = 2.05950(2) Å [10]; b_o = 2.072(5) Å [16]. The obtained ratio b_o/b_t = 1.039 is smaller than the one corresponding to an ideal spinel (b_o/b_t(ideal) = 1.155). This result implies an increase in the size of the tetrahedral sites at the expense of the octahedral ones. The observed changes in the site sizes are due mainly to the distribution of Zn^{2+} and Li^+ and the difference in the effective ionic radius [33].

4. Conclusions

Doping $Zn_{7/3}Sb_{2/3}O_4$ with Li^+ introduces slight modifications of its spinel structure. Mentioned variations have been investigated by taking full advantage of experiments with synchrotron radiation and neutrons. Synchrotron light allowed high resolution measurement of the cubic cell parameter. Neutrons led to the determination of the coordination polyhedra changes and sites' occupancies, including Li^+ ions' distribution. Zn^{+2} ions are partly replaced by Sb^{+5} and Li^+ in octahedral sites and by Li^+ in tetrahedral sites.

The present structure analysis represents a configurational basis for first principles calculations, leading to quantitative interpretation of experimental results, related with thermo-electrical and optical properties of the considered materials, results which publication is being prepared.

Acknowledgments: Authors are grateful to the Institut Laue-Langevin and to Elettra Sincrotrone Trieste and to the International Centre for Theoretical Physics for ample support to the performed research. Special Thanks to M.C.D. Huerta and Ing. W. Cauich for the technical assistance with SEM images and XPS measurements respectively. This work was supported by Conacyt project no. CB178947 and the grant given to J.A. Marín-Romero (No. 251144).

Author Contributions: José Alfredo Marín Romero, Luis Edmundo Fuentes Cobas, Juan Rodriguez-Carvajal and Patricia Quintana conceived and designed the experiments; Luis Edmundo Fuentes Cobas performed the experiments in synchrotron; José Alfredo Marín-Romero and Juan Rodríguez-Carvajal performed the experiments of neutron diffraction and analyzed data; Luis Edmundo Fuentes Cobas, Patricia Quintana Owen and José Alfredo Marín Romero analyzed the data and wrote the paper; Patricia Quintana contributed reagents/materials/analysis tools; Carolina Tabasco Novelo prepared the samples and the analysis on XPS; Patricia Quintana is the leader of the project.

Conflicts of Interest: The authors declare no conflict of interest.

References

1. Talanov, V.M. Calculation of Structural Parmeters of Spinels. *Phys. Status Solidi* **1981**, *106*, 99–106. [CrossRef]
2. Talanov, V.M. Structural Modelling of Low-Symmetry Phases of Spinels. I. Phases with 1:1 Octahedral Order. *Phys. Status Solidi* **1990**, *162*, 61–73. [CrossRef]
3. Biagioni, C.; Pasero, M. The systematics of the spinel-type minerals: An overview. *Am. Mineral.* **2014**, *99*, 1254–1264. [CrossRef]
4. Sickafus, K.E.; Wills, J.M.; Grimes, N.W. Structure of Spinel. *J. Am. Ceram. Soc.* **1999**, *82*, 3279–3292. [CrossRef]
5. Yuan, C.; Wu, H.B.; Xie, Y.; Lou, X.W. Mixed transition-metal oxides: Design, synthesis, and energy-related applications. *Angew. Chem. Int. Ed.* **2014**, *53*, 1488–1504. [CrossRef] [PubMed]
6. Lisboa-Filho, P.N.; Vila, C.; Góes, M.S.; Morilla-Santos, C.; Gama, L.; Longo, E.; Schreiner, W.H.; Paiva-Santos, C.O. Composition and electronic structure of $Zn_{7-x}M_xSb_2O_{12}$ (M=Ni and Co) spinel compounds. *Mater. Chem. Phys.* **2004**, *85*, 377–382. [CrossRef]
7. Bernik, S.; Branković, G.; Rustja, S.; Žunić, M.; Podlogar, M.; Branković, Z. Microstructural and compositional aspects of ZnO-based varistor ceramics prepared by direct mixing of the constituent phases and high-energy milling. *Ceram. Int.* **2008**, *34*, 1495–1502. [CrossRef]
8. Branković, Z.; Branković, G.; Poleti, D.; Varela, J. Structural and electrical properties of ZnO varistors containing different spinel phases. *Ceram. Int.* **2001**, *27*, 115–122. [CrossRef]
9. Huang, Y.; Liu, M.; Zeng, Y.; Li, C. The effect of secondary phases on electrical properties of ZnO-based ceramic films prepared by a sol-gel method. *J. Mater. Sci. Mater. Electron.* **2004**, *5*, 549–553. [CrossRef]
10. Harrington, R.; Miles, G.C.; West, A.R. Phase equilibria, crystal chemistry and polymorphism of $Zn_7Sb_2O_{12}$ doped with Cr and Ni. *Mater. Res. Bull.* **2008**, *43*, 1949–1956. [CrossRef]
11. Harrington, R.; Miles, G.C.; West, A.R. Crystallography of Ni-doped $Zn_7Sb_2O_{12}$ and phase equilibria in the system ZnO-Sb_2O_5-NiO. *J. Eur. Ceram. Soc.* **2006**, *26*, 2307–2311. [CrossRef]
12. Miles, G.C.; West, A.R. Polymorphism and Thermodynamic Stability of $Zn_7Sb_2O_{12}$. *J. Am. Ceram. Soc.* **2005**, *88*, 396–398. [CrossRef]
13. Filipek, E.; Dąbrowska, G. Phase relations up to the solidus line in the part of the Sb-Zn-O system. *Open Chem.* **2009**, *7*, 192–196. [CrossRef]
14. Kuramochi, K.; Suzuki, K.; Yamazaki, T.; Mitsuishi, K.; Furuya, K.; Hashimoto, I.; Watanabe, K. Quantitative structural analysis of twin boundary in using {HAADF} {STEM} method. *Ultramicroscopy* **2008**, *109*, 96–103. [CrossRef] [PubMed]
15. Talanov, V.M.; Shirokov, V.B. Tilting structures in spinels. *Acta Crystallogr. Sect. A Found. Crystallogr.* **2012**, *68*, 595–606. [CrossRef] [PubMed]
16. Harrington, R.; Miles, G.C.; West, A.R. Crystal chemistry of Co-doped $Zn_7Sb_2O_{12}$. *J. Solid State Chem.* **2008**, *181*, 334–339. [CrossRef]
17. Braun, P.B. A Superstructure in Spinels. *Nature* **1952**, *170*, 1123. [CrossRef]

18. Houabes, M.; Metz, R. The effect of lithium oxide on the threshold field of ZnO varistors. *Ceram. Int.* **2009**, *35*, 1385–1389. [CrossRef]
19. Clarke, D.R. Varistor Ceramics. *J. Am. Ceram. Soc.* **2004**, *82*, 485–502. [CrossRef]
20. Meyer, B.K.; Stehr, J.; Hofstaetter, A.; Volbers, N.; Zeuner, A.; Sann, J. On the role of group I elements in ZnO. *Appl. Phys. A.* **2007**, *88*, 119–123. [CrossRef]
21. Rodríguez-Carvajal, J. Recent advances in magnetic structure determination by neutron powder diffraction. *Phys. B Condens. Matter* **1993**, *192*, 55–69. [CrossRef]
22. Fuentes-Cobas, L.E. Synchrotron Radiation Diffraction and Scattering in Ferroelectrics. In *Multifunctional Polycrystalline Ferroelectric Materials*; Springer: Dordrecht, The Netherlands, 2011; pp. 217–280.
23. Lutterotti, L.; Bortolotti, M.; Ischia, G.; Lonardelli, I.; Wenk, H.R. Rietveld texture analysis from diffraction images. *Z. Krist. Suppl.* **2007**, *1*, 125–130. [CrossRef]
24. Young, R.A. *The Rietveld Method. International Union of Crystallography Monographs on Crystallography*; Oxford University Press: Oxford, UK, 1993.
25. Delacourt, C.; Rodríguez-Carvajal, J.; Schmitt, B.; Tarascon, J.M.; Masquelier, C. Crystal chemistry of the olivine-type Li_xFePO_4 system ($0 \leq x \leq 1$) between 25 and 370°C. *Solid State Sci.* **2005**, *7*, 1506–1516. [CrossRef]
26. Wang, J.; Peng, G.; Guo, Y.; Yang, X. XPS investigation of segregation of Sb in SnO_2 powders. *J. Wuhan Univ. Technol. Mater. Sci. Ed.* **2008**, *23*, 95–99. [CrossRef]
27. Gurgul, J.; Rinke, M.T.; Schellenberg, I.; Pöttgen, R. The antimonide oxides REZnSbO and REMnSbO (RE = Ce, Pr)-An XPS study. *Solid State Sci.* **2013**, *17*, 122–127. [CrossRef]
28. Wagner, C.D.; Davis, L.E.; Zeller, M.V.; Taylor, J.A.; Raymond, R.H.; Gale, L.H. Empirical atomic sensitivity factors for quantitative analysis by electron spectroscopy for chemical analysis. *Surf. Interface Anal.* **1981**, *3*, 211–225. [CrossRef]
29. Redhammer, G.J.; Tippelt, G. Crystal structure of spinel-type $Li_{0.64}Fe_{2.15}Ge_{0.21}O_4$. *Acta Crystallogr. Sect. E Crystallogr. Commun.* **2016**, *72*, 505–508. [CrossRef] [PubMed]
30. Ezhilvalavan, S.; Kutty, T.R.N. Low-voltage varistors based on zinc antimony spinel $Zn_7Sb_2O_{12}$. *Appl. Phys. Lett.* **1996**, *68*, 2693–2695. [CrossRef]
31. Momma, K.; Izumi, F. VESTA 3 for three-dimensional visualization of crystal, volumetric and morphology data. *J. Appl. Crystallogr.* **2011**, *44*, 1272–1276. [CrossRef]
32. O'Neill, H.S.C.; Navrotsky, A. Simple spinels; crystallographic parameters, cation radii, lattice energies, and cation distribution. *Am. Mineral.* **1983**, *68*, 181–194.
33. Shannon, R.D.; Prewitt, C.T. Effective ionic radii in oxides and fluorides. *Acta Crystallogr. Sect. B Struct. Crystallogr. Cryst. Chem.* **1969**, *25*, 925–946. [CrossRef]